Organic & Biomolecular Chemistry

ROYAL SOCIETY OF CHEMISTRY

PAPER

View Article Online
View Journal | View Issue

Cite this: *Org. Biomol. Chem.*, 2025, **23**, 4675

Inhibition of acrylic acid and acrylate autoxidation†

Onkar S. Nayal,‡[a] Oleg Grossmann[b] and Derek A. Pratt *[a]

Received 13th February 2025,
Accepted 8th April 2025

DOI: 10.1039/d5ob00265f

rsc.li/obc

Acrylic acid (AA) is a versatile monomer whose high reactivity can present a challenge for transport and storage due to its highly exergonic oligomerization, which can lead to runaway polymerization and explosion. To prevent premature polymerization of acrylic acid, hydroquinone monomethyl ether (MeHQ) and phenothiazine (PTZ) are commonly used as inhibitors/stabilizers. Despite their widespread use, the limited radical-trapping stoichiometry of MeHQ and oxidative consumption of PTZ at process temperatures are clear limitations. Herein, we apply a recently devised spectrophotometric approach employing the autoxidizable STY-BODIPY dye to monitor reaction progress in autoxidations of acrylic acid, *n*-butyl acrylate and the non-polymerizable 2-ethylhexanol, and the impact of a panel of radical-trapping antioxidants (RTAs, including MeHQ and PTZ) upon them. We find that the radical-trapping stoichiometry is highly substrate-dependent, with nitroxides and aromatic amines that can be converted to nitroxides *in situ* exhibiting superstoichiometric activities in substrates where hydroperoxyl radicals are formed or in the presence of acid. *N*-Alkyl derivatives of phenoxazine, the most potent RTA uncovered to date, are found to be particularly excellent inhibitors of AA autoxidation. It is proposed that gradual acid-mediated dealkylation to phenoxazine minimizes accumulation of the phenoxazine-derived nitroxide, which can otherwise undergo acid-catalyzed disproportionation and diminish radical-trapping capacity. These results suggest that *N*-alkylated phenoxazine derivatives should be explored further as stabilizers of AA.

Introduction

Acrylic acid (AA) and its esters are versatile vinyl monomers used as building blocks for thousands of polymer formulations.[1] As one of the fastest-growing monomer markets, AA demand stood at 6.7 million tonnes in 2022 and is expected to grow at a compound annual growth rate of 4.39% through 2032.[2] AA is a very reactive monomer that can undergo spontaneous and highly exergonic polymerization.[3] As a result, a major challenge associated with AA production and storage is runaway polymerization. Indeed, several serious accidents have been reported over the years, including explosions at the Fu-Kao plant in Taiwan in 2001 and the Himeji plant of Nippon Shokubai in Japan in 2012.[4–6] Even when not progressing to this devastating stage, premature polymerization can lead to reactor/transport blockages which negatively impact the efficiency of a production plant and raise costs.

Vinyl monomers such as AA and its esters are excellent substrates for radical chain reactions: radical polymerization in the absence of O_2 and autoxidation in the presence of O_2.[7–9] While polymerization propagates by successive addition of the propagating carbon-centred macroradical to monomer, autoxidation involves combination of the carbon-centred (macro)radical with O_2 to yield a peroxyl radical, followed by addition of the peroxyl (macro)radical to monomer yielding an alternating co-polymer of monomer and O_2 units (Fig. 1A). Since the propagation of autoxidation is generally much slower than of polymerization, O_2 itself can be viewed as a polymerization inhibitor. However, the peroxidic linkages introduced in the copolymer are thermally labile, and upon O–O bond cleavage, further radical chain reactions are initiated enabling the premature or runaway polymerization processes mentioned above. Thus, control of O_2 and/or autoxidative processes is vital to monomer/polymer quality and safety.

Hydroquinone monomethyl ether (MeHQ) and phenothiazine (PTZ) are commonly used inhibitors/stabilizers.[10,11] MeHQ and PTZ are examples of phenolic and aminic radical-trapping antioxidants (RTAs), respectively, which inhibit polymerization/autoxidation by reacting with chain-propagating radicals.[12] Independent studies by Levy[13] and Vogel[14] suggest that MeHQ is an effective inhibitor of AA polymeriz-

[a]*Department of Chemistry and Biomolecular Sciences, University of Ottawa, 10 Marie Curie Pvt., Ottawa, Ontario, K1N 6N5, Canada. E-mail: dpratt@uottawa.ca*
[b]*Group Research, BASF SE, Ludwigshafen, Germany*

†Electronic supplementary information (ESI) available. See DOI: https://doi.org/10.1039/d5ob00265f

‡Current address: Department of Chemistry, Amity Institute of Applied Sciences, Amity University, Noida, Uttar Pradesh, India.

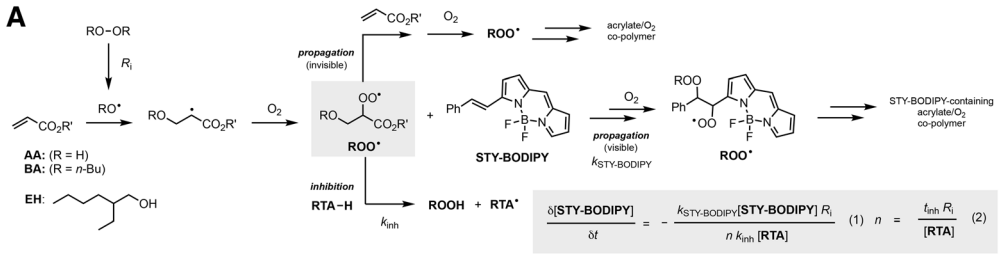

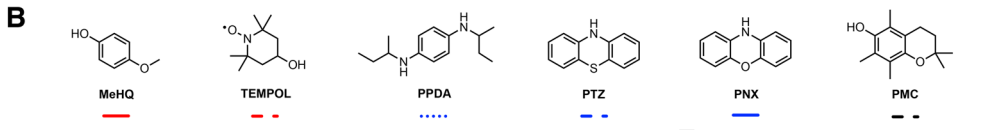

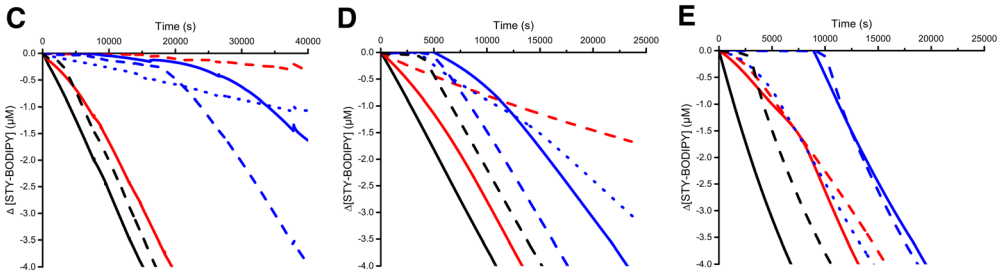

F

	k_{inh} ($M^{-1}s^{-1}$)			n		
	EH	BA	AA	EH	BA	AA
MeHQ	$2.0 \pm 0.6 \times 10^5$	$1.7 \pm 0.1 \times 10^4$	$2.9 \pm 0.5 \times 10^4$	2.9 ± 0.8	2.2 ± 0.3	3.4 ± 0.4
TEMPOL	$2.1 \pm 0.8 \times 10^6$	$5.2 \pm 1.2 \times 10^4$	$4.6 \pm 1.1 \times 10^4$	>20	>2	n.d.
PPDA	$1.5 \pm 0.5 \times 10^6$	$6.4 \pm 0.6 \times 10^5$	$5.7 \pm 0.6 \times 10^4$	>20	>2	3.0 ± 0.2
PTZ	$2.2 \pm 1.2 \times 10^6$	$>10^6$	$2.8 \pm 0.7 \times 10^6$	15.4 ± 0.5	>2.6 ± 0.2	6.6 ± 0.7
PNX	$4.9 \pm 1.5 \times 10^6$	$>10^6$	$>3 \times 10^6$	>19.1	>2.9	5.7 ± 0.3
PMC	$8.2 \pm 0.5 \times 10^5$	$3.0 \pm 0.6 \times 10^5$	$2.1 \pm 0.1 \times 10^5$	2	2	2

Fig. 1 (A) General scheme for the peroxide-initiated autoxidation of acrylic acid and butyl acrylate and illustration of the STY-BODIPY co-autoxidation approach. (B) Structures of inhibitors investigated in this work. (C)–(E). Representative co-autoxidations of EH (C), BA (D) and AA (E) (2.91 M) and STY-BODIPY (10 μM) initiated by di-*tert*-butylperoxide (295 mM) in chlorobenzene at 70 °C (black line) and inhibited by either 6 μM (C), 12 μM (D) or 24 μM (E) of the compounds shown in panel B. STY-BODIPY consumption was monitored by absorbance at 568 nm (ε = 117 736 M^{-1} cm^{-1}), 569 nm (D, ε = 107 571 M^{-1} cm^{-1}) and 572 nm (E, ε = 118 469 M^{-1} cm^{-1}). (F) Calculated inhibition rate constants and radical-trapping stoichiometries determined by eqn (1) and (2).

ation at ambient temperatures in the presence of O_2 while PTZ is additionally highly efficient in trapping thermally generated alkyl radicals in the absence of O_2. As a result, MeHQ is commonly used as a stabilizer for transport and PTZ is used as a stabilizer during the distillation and purification of acrylic acid.[14] Despite their widespread use, the limited radical-trapping stoichiometry of MeHQ and the increased oxidative consumption of PTZ at process temperatures limit the applicability of these stabilizers.[10,11]

Some time ago our group introduced an approach to monitor autoxidation progress and the impact of RTAs upon it indirectly using the coloured co-autoxidizable substrate STY-BODIPY (Fig. 1A).[15] This approach circumvents the need for specialized sophisticated instruments to monitor autoxidation progress, and instead requires only a spectrophotometer to determine consumption of STY-BODIPY over time as it undergoes co-autoxidation with the substrate. Since the rate constant of the reaction of STY-BODIPY with chain-carrying peroxyl radicals can be determined independently, both the inhibition rate constant (k_{inh}) and radical-trapping stoichiometry (n) of added RTAs can be readily determined from the initial rates of STY-BODIPY consumption and inhibited periods, respectively, using standard formulae (eqn (1) and (2), Fig. 1A inset).[16] Thus, despite its simplicity, this approach provides robust quantitative information about RTA activity – a trait which is not shared by other spectrophotometric antioxidant assays such as those which use DPPH and ABTS.[17,18] Herein we utilize this approach to provide insight on the mechanisms by which MeHQ and PTZ inhibit the autoxidation of AA and its esters in order to enable the identification of new approaches to improve both safety and economics.

Results and discussion

Inhibited co-autoxidations of 2-ethylhexanol, *n*-butyl acrylate and acrylic acid

Co-autoxidations of STY-BODIPY and each of AA, *n*-butyl acrylate (BA) and 2-ethylhexanol (EH) were carried out in the presence of a panel of RTAs (Fig. 1B). EH was chosen as a representative non-polymerizable substrate and happens to be esterified to AA in many commercial products. In addition to the aforementioned conventional stabilizers of AA (MeHQ and PTZ), we investigated the aromatic amines phenoxazine (PNX) and *N*,*N*′-di-*sec*-butylbenzene-1,4-diamine (PPDA), the nitroxide 4-hydroxyTEMPO (TEMPOL) and 2,2,5,7,8-pentamethylchroman-6-ol (PMC), the reactive phenolic headgroup of α-tocopherol, the most potent form of Vitamin E.[19] Representative data for inhibited co-autoxidations of EH, BA, and AA are shown in Fig. 1C, D and E, respectively. Tabulated below them in Fig. 1F are the corresponding values of k_{inh} for each of the inhibitors, derived from the initial rates using eqn (1), as well as the radical-trapping stoichiometries, derived from the inhibited periods using eqn (2).

The use of eqn (1) to derive k_{inh} requires knowledge of $k_{STY\text{-}BODIPY}$, which was determined from the rate of STY-BODIPY consumption in uninhibited autoxidations as a function of STY-BODIPY consumption to be 10 010 M^{-1} s^{-1}, 1544 M^{-1} s^{-1} and 1785 M^{-1} s^{-1} in EH, BA and AA, respectively (see ESI†).[8,20] Likewise, the use of eqn (2) to derive n requires knowledge of the rate of radical initiation, R_i, which was determined from the duration of the inhibited period observed in the presence of PMC, since PMC is known to trap 2 peroxyl radicals.[19]

In the EH co-autoxidations, there was a marked difference between the phenolic and aminic RTAs. PMC and MeHQ were characterized by relatively short inhibited periods corresponding to $n \sim 2$, while PTZ, PNX and PPDA exhibited inhibited periods corresponding to $n > 15$, with PNX and PPDA still retarding the autoxidation beyond the end of the nominal inhibited periods. Most interestingly, TEMPOL inhibited the autoxidation for the duration of the experiment. Consistent with their reactivity in other autoxidizable hydrocarbons,[21] PMC was roughly one order of magnitude more reactive than MeHQ and each of the aromatic amines were more reactive than PMC.[22]

Inhibited co-autoxidations of BA afforded similar trends, with the amines generally outperforming the phenols, but by a lesser margin with respect to radical-trapping stoichiometries. In this medium there was also a clear difference between the amines and TEMPOL, which does not show an inhibited period – consistent with a much lower k_{inh} – but retards the autoxidation for the duration of the experiment. PPDA also retards beyond the initial inhibited period, whereas the autoxidations in the presence of PNX and PTZ return to the uninhibited rate at the end of the inhibited period.

Moving to AA, the phenols again displayed the poorest performance, with the lowest radical-trapping stoichiometries, followed by PPDA and TEMPOL and then PNX and PTZ. The trends in inhibition rate constants derived from the initial rates nevertheless remained more or less the same (*i.e.* PTZ ~ PNX > TEMPOL > PPDA > MeHQ) – except for TEMPOL which now showed better activity from the outset relative to its performance in BA. It is noteworthy that the STY-BODIPY co-autoxidation method can also report on gelation times in the same experiment, as the increase in optical density upon polymerization leads to a rapid increase in absorbance once STY-BODIPY (and O_2) has been largely consumed (see ESI for examples†). However, since our interest is in the inhibition of the autoxidation of the monomers to peroxidic species, our focus is on the reaction progress long before sample gelation.

Probing for hydroperoxyl radical chemistry as a function of substrate

The substrate dependence of the RTA activity observed above suggests that different reaction mechanisms are at play in the different substrates. The very clear differences between phenolic and aminic RTAs in the non-polymerizable EH, with the latter affording very large radical-trapping stoichiometries while the former follow the conventional $n \sim 2$, is reminiscent of observations made when hydroperoxyl radicals (HOO$^\bullet$) are formed during chain propagation.[23–25] This has been most thoroughly investigated for unsaturated substrates, where 1,4-HAT in an alkylperoxyl radical intermediate (resulting from radical addition and combination with O_2) is followed by elimination to produce HOO$^\bullet$.[25] While EH lacks unsaturation, ketyl radicals – such as that resulting from HAT from C1 of EH – are known to react with O_2 to yield HOO$^\bullet$.[26–28] The intervention of HOO$^\bullet$ is most clearly indicated when nitroxides, such as TEMPO, perpetually inhibit the autoxidation,[25,29] as is the case for TEMPOL in EH. This arises due to the near diffusion-controlled H-atom transfer from HOO$^\bullet$ to TEMPO, which yields O_2 and TEMPOH, a hydroxylamine.[25] TEMPOH then reacts with a peroxyl radical to inhibit the autoxidation and reform TEMPO in what is formally a nitroxide-catalyzed cross-dismutation of HOO$^\bullet$ and ROO$^\bullet$. Since the aromatic amines PPDA, PNX and PTZ can all be converted to nitroxides *in situ*, they also inhibit with very high radical-trapping stoichiometry. The fact that PTZ has the lowest stoichiometry is consistent with our recent finding that its nitroxide reacts with PTZ to yield the PTZ sulfoxide (and PTZ-derived aminyl radical).[30]

In order to provide further evidence that HOO$^\bullet$ is formed in the autoxidation of EH, the isomeric hydroquinones 3,5-di-*tert*-butylcatechol and 2,5-di-*tert*-butylhydroquinone and their corresponding quinones were also investigated as RTAs as shown in Fig. 2. Similarly to nitroxides, *o*-quinones can be reduced *in situ* to form potent RTAs, (Fig. 2A) while *p*-quinones which lack H-bonding stabilization in the intermediate semiquinone radicals are comparatively unreactive (Fig. 2B).[31] Indeed, we found the catechol and *o*-quinone to have similar reactivity in EH ($k_{inh} = 1.6 \times 10^6$ and 1.2×10^6 M^{-1} s^{-1}, respectively) with very large radical-trapping stoichiometries ($n > 12.6$ and 12.0, respectively) consistent with reduction of the *o*-quinone (and/or its semiquinone) by HOO$^\bullet$ formed *in situ* (Fig. 2C). By comparison the hydroquinone only retarded the

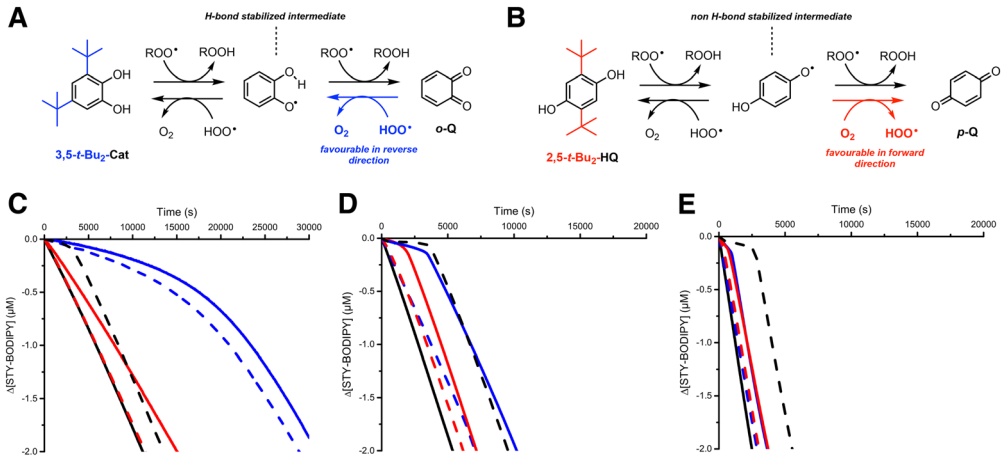

F

	k_{inh} ($M^{-1}s^{-1}$)			n		
	EH	BA	AA	EH	BA	AA
3,5-*t*-Bu_2-Cat	$1.6 \pm 0.3 \times 10^6$	$1.1 \pm 0.8 \times 10^5$	$3.9 \pm 0.6 \times 10^4$	>12.6 ± 0.3	> 2.0 ± 0.4	0.7 ± 0.4
3,5-*t*-Bu_2-*o*-Q	$1.2 \pm 0.2 \times 10^6$	$1.5 \pm 0.3 \times 10^4$	n.d.	>12.0 ± 0.6	n.d.	n.d.
2,5-*t*-Bu_2-HQ	$1.8 \pm 0.4 \times 10^5$	$7.7 \pm 1.2 \times 10^4$	$2.5 \pm 0.7 \times 10^4$	n.d.	1.0 ± 0.2	0.6 ± 0.2
2,5-*t*-Bu_2-*p*-Q	n.d.	$1.3 \pm 0.2 \times 10^4$	n.d.	n.d.	n.d.	n.d.

Fig. 2 (A) Semiquinone radicals derived from catechols are stabilized by an intramolecular H-bond, which strengthens the O–H bond and enables reduction of *o*-quinones by hydroperoxyl radicals. (B) Semiquinones radicals derived from hydroquinones lack the stabilization due to H-bonding and undergo competitive reactions with O_2 to form the *p*-quinone. (C)–(E) Representative co-autoxidations of EH (C), BA (D) and AA (E) (2.91 M) and STY-BODIPY (10 μM) initiated by di-*tert*-butylperoxide (295 mM) in chlorobenzene at 70 °C (black line) and inhibited by 6 μM of either 3,5-*t*-Bu_2-Cat or 2,5-*t*-Bu_2-HQ (blue and red solid lines), their corresponding quinones (blue and red dashed lines) or PMC (black dashed lines). STY-BODIPY consumption was monitored by absorbance at 568 nm (C, ε = 117 736 M^{-1} cm^{-1}), 569 nm (D, ε = 107 571 M^{-1} cm^{-1}) and 572 nm (E, ε = 118 469 M^{-1} cm^{-1}). (F) Calculated inhibition rate constants and radical-trapping stoichiometries determined by eqn (1) and (2).

autoxidation and the corresponding *p*-quinone was devoid of activity.

In BA, the catechol clearly trapped two radicals, while the hydroquinone trapped less than one (Fig. 2D). Moreover, the catechol continued to retard the autoxidation very slightly following the end of the inhibited periods, while PMC and the hydroquinone did not. The *o*-quinone retarded at essentially the same rate as the catechol following the inhibited period, while the *p*-quinone was essentially devoid of activity. Thus, overall, the trends are similar to those in EH, pointing to a role for HOO• formation during BA autoxidation, but to a far lesser extent than in EH – perhaps in part due to the greater oxidizability of BA relative to EH. HOO• formation from the ketyl radical in EH is likely a good competitor with propagation relative to the 1,4-HAT pathway characterized for HOO• formation from unsaturated substrates particularly since HAT involves a less hydridic C–H bond in BA compared to the substrates previously shown to engage this chemistry (*e.g.* styrene, norbornene, hexadecene).[25]

In stark contrast, we could find no evidence for HOO• formation in AA co-autoxidations using the (hydro)quinones. While the quinones were essentially devoid of activity, the hydroquinones gave rise to short inhibited periods corresponding to $n < 1$ followed by uninhibited autoxidations (see Fig. 2E). These results appear consistent with the observations made for the panel of test RTAs in Fig. 1C–E, where they performed very differently in AA as compared to BA and EH. That is, none of the compounds indefinitely retarded the autoxidation, and instead, each of the inhibited autoxidations were marked by well-defined inhibited and uninhibited phases. PTZ and PNX were now the best performing compounds, followed by TEMPOL and PPDA and, finally, the phenols. Interestingly, despite the apparent lack of HOO• formation, the amines/nitroxide continue to display radical-trapping stoichiometries greater than 2, implying some 'catalytic' radical-trapping process. At first glance, the fact that HOO• formation occurs in BA — but not AA — implies an involvement of the butyl side chain, but it is more likely that this is simply because the intramolecular process leading to HOO• cannot compete with the faster propagation in AA.

Catalytic radical-trapping in acrylic acid autoxidation

Catalytic radical-trapping by PTZ in autoxidations of AA has been reported previously. Levy[32] suggested the mechanism in Fig. 3A, where monomeric or polymeric alkyl or peroxyl radicals of AA are proposed to be reduced by single-electron transfer (SET) to form the corresponding anion and a PTZ radical cation. H-atom transfer (HAT) from a monomeric or polymeric alkyl radical of AA to the PTZ radical cation was proposed to

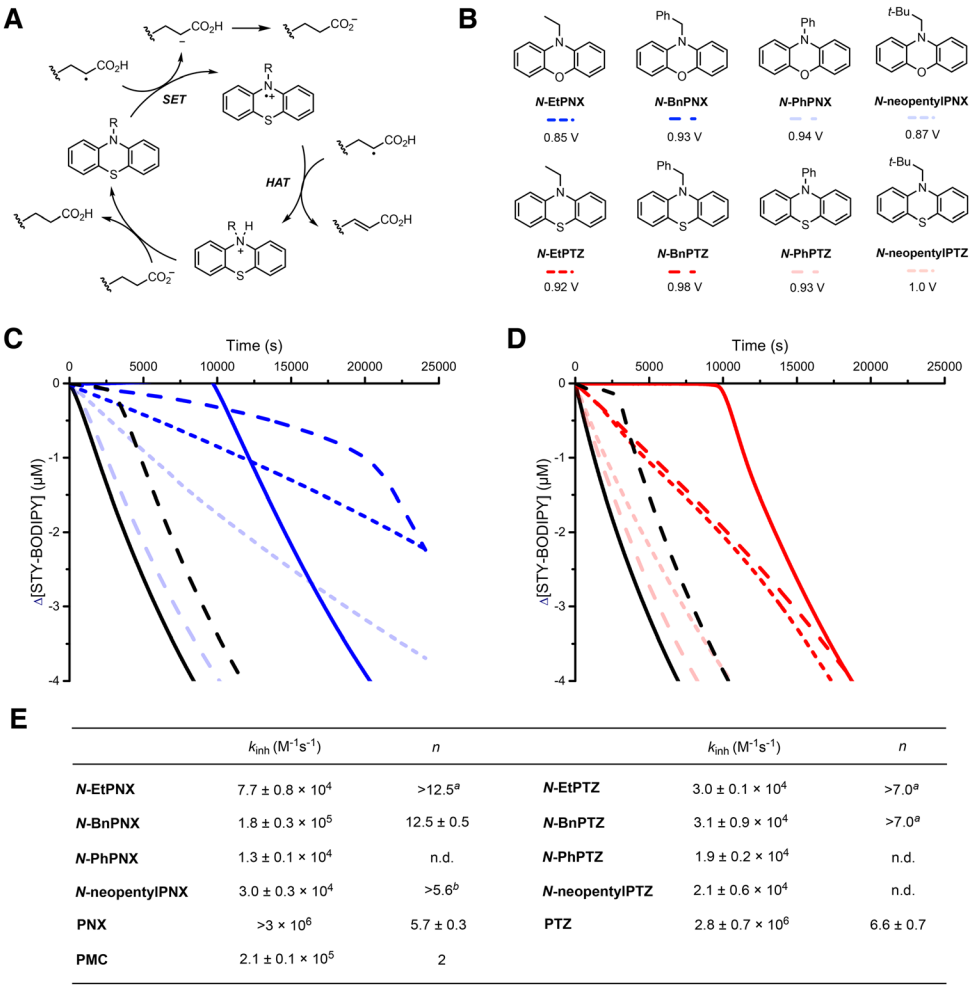

E

	k_{inh} ($M^{-1}s^{-1}$)	n		k_{inh} ($M^{-1}s^{-1}$)	n
***N*-EtPNX**	$7.7 \pm 0.8 \times 10^4$	>12.5[a]	***N*-EtPTZ**	$3.0 \pm 0.1 \times 10^4$	>7.0[a]
***N*-BnPNX**	$1.8 \pm 0.3 \times 10^5$	12.5 ± 0.5	***N*-BnPTZ**	$3.1 \pm 0.9 \times 10^4$	>7.0[a]
***N*-PhPNX**	$1.3 \pm 0.1 \times 10^4$	n.d.	***N*-PhPTZ**	$1.9 \pm 0.2 \times 10^4$	n.d.
***N*-neopentylPNX**	$3.0 \pm 0.3 \times 10^4$	>5.6[b]	***N*-neopentylPTZ**	$2.1 \pm 0.6 \times 10^4$	n.d.
PNX	$>3 \times 10^6$	5.7 ± 0.3	**PTZ**	$2.8 \pm 0.7 \times 10^6$	6.6 ± 0.7
PMC	$2.1 \pm 0.1 \times 10^5$	2			

Fig. 3 (A) Catalytic radical-trapping cycle proposed by Levy. (B) *N*-Alkylated and *N*-arylated PNX and PTZ derivatives investigated as inhibitors of AA autoxidation and their corresponding oxidation potentials as determined by cyclic voltammetry in CH_3CN containing Bu_4NPF_6 (see ESI† for corresponding voltammagrams). (C and D). Representative co-autoxidations of AA (2.91 M) and STY-BODIPY (10 μM) initiated by di-*tert*-butylperoxide (295 mM) in chlorobenzene at 70 °C (black line) and inhibited by 24 μM *N*-substituted PNX (C) and PTZ (D) derivatives shown in panel B or PMC (black dashed lines). STY-BODIPY consumption was monitored by absorbance at 572 nm (ε = 118 469 M^{-1} cm^{-1}). (E) Calculated inhibition rate constants and radical-trapping stoichiometries determined by eqn (1) and (2). Corresponding data for PNX (blue solid line) and PTZ (red solid line) are from Fig. 1.

follow, where PTZ was then regenerated following proton transfer.

While this mechanism has been espoused by others,[33] we find it difficult to reconcile our results in its light. First, since our experiments are carried out under O_2, it is expected that PTZ will react with peroxyl radicals and not alkyl radicals. Although PTZ is a good one-electron donor (E° = 0.85 V *vs.* NHE), it has been shown to react with peroxyl radicals by HAT.[34] Importantly, the value of k_{inh} for PTZ determined in AA at 70 °C (2.8×10^6 M^{-1} s^{-1}) is smaller than that determined at 50 °C in benzene ($k_{inh} = 8.8 \times 10^6$ M^{-1} s^{-1}); were SET to be the mechanism of the reaction, k_{inh} should be greater in the more polar AA as compared to benzene. Instead, if HAT were operative, it is expected to be roughly 10-fold slower in AA than benzene since AA is a better H-bond acceptor than benzene ($\Delta\beta_2^H = 0.31$)[35] for PTZ ($\Delta\alpha_2^H = 0.38$)[36,37] – consistent with our observations (particularly in light of the fact that our experiments were done at 70 °C instead of 50 °C). Second, the regeneration of PTZ from its radical cation is proposed to occur *via* HAT from a chain-propagating alkyl radical. Not only is HAT from a C–H bond a relatively slow reaction,[38] but alkyl radicals do not accumulate due to their near diffusion-controlled reaction with O_2.[39] Consider that even if PTZ was quantitatively converted to its radical cation, it would have to react with the propagating radical >40-fold faster than O_2 (given the concentration difference of ~24 μM and ~1 mM) which would require a rate constant well in excess of that limited by diffusion!

Subsequent work by Matyjaszewski found some *N*-alkylated PTZ derivatives were better able to prevent AA autoxidation/polymerization than PTZ.[33] At first glance, these observations support Levy's mechanism, since no HAT is possible from the *N*-alkylated derivatives. To provide additional insight on the

mechanism, we sought to confirm these trends in our system and determine whether PNXs are characterized by the same substituent effect. Thus, we synthesized *N*-benzylated and *N*-ethylated PNX and PTZ (structures shown among others in Fig. 3B) and tested their efficacy as inhibitors of AA autoxidation as shown in Fig. 3C and D.

The autoxidations inhibited by *N*-alkylated PTZ and PNX derivatives were characterized by faster rates of STY-BODIPY consumption compared to those inhibited by PTZ and PNX, but were retarded for far longer, consistent with Matyjaszewski's results.[33] The slower inhibition kinetics are consistent with the expectedly slower reactivity of the *N*-alkylated derivatives with propagating radicals than those of the free amines under the experimental conditions. However, the fact that the *N*-alkylated derivatives continue to retard the oxidation well beyond the parent amines was highly intriguing. Moreover, while PTZ had a marginally longer inhibited period than PNX, the *N*-alkylated PNXs were demonstrably better inhibitors than the corresponding *N*-alkylated PTZs.

To expand on these structure–reactivity relationships, we prepared *N*-PhPNX and *N*-PhPTZ and evaluated their reactivity in AA (also shown in Fig. 3C and D). Despite the fact that *N*-PhPNX has a practically indistinguishable oxidation potential from *N*-BnPNX (E° = 0.93 V and 0.94 V, respectively) and *N*-PhPTZ is more easily oxidized than *N*-BnPTZ (E° = 0.93 V and 0.98 V, respectively), the *N*-phenylated derivatives were essentially devoid of activity. This suggests that initial electron transfer to a propagating radical and formation of the PTZ/PNX radical cation is not operative.

Since the ethyl/benzyl groups could, in principle, be cleaved under acidic conditions, but the phenyl group would not, we considered that acid-catalyzed dealkylation could reveal highly reactive PNX/PTZ *in situ*. Thus, we carried out inhibited autoxidations of BA and EH in the presence of the *N*-alkylated PNX derivatives where no acid-catalyzed dealkylation could occur. Indeed, under these conditions, both the *N*-alkylated and *N*-arylated PNX derivatives were essentially devoid of activity (Fig. 4A). However, upon addition of acetic acid to the media, much of the reactivity of the *N*-EtPNX and *N*-BnPNX was restored (Fig. 4B). Clearly, acid is required for highly efficient inhibitory activity of the *N*-alkylated PNX/PTZ – a requirement not readily explained by Levy's mechanism.

To confirm that the *N*-alkylated PNX/PTZ could be dealkylated under the reaction conditions, we incubated *N*-BnPNX in acetic acid at 70 °C. To our surprise, no debenzylation was observed within 24 hours – a period far in excess of the duration of our inhibited autoxidation experiments. Since the only other difference between these reaction conditions and the autoxidation conditions were propagating radicals, we included AIBN alongside acetic acid and readily observed PNX and the primary product of its oxidative dimerization in good yields (55% following column chromatography, see ESI†).

Given the requirement for both acid and propagating radicals in the dealkylation process, we envisioned two possible mechanisms as shown in Fig. 4C. The first involves initial HAT to give an aminoalkyl radical followed by SET to form an iminium ion that could be hydrolyzed/alcoholized to give the amine. The second involves the opposite sequence: initial SET to give a radical cation followed by HAT to form the iminium ion. Since Lucarini and co-workers estimate a paltry 60 M^{-1} s^{-1} for the reaction of peroxyl radicals with *N*-MePTZ, precluding the possibility that it will compete with chain propagation, the second option is more likely.[36] Indeed, PTZ and PNX radical cations are known to be fairly persistent,[40] enabling them to accumulate to react with another peroxyl radical. However, given this premise, we may have expected *N*-PhPNX/*N*-PhPTZ to inhibit AA autoxidation – unless SET is reversible, and a subsequent HAT is necessary to render it irreversible. Indeed, when we carried out autoxidations inhibited by a deuterated analog of *N*-EtPNX (*i.e.* *N*-C_2D_5PNX), a kinetic isotope effect was observed (k_H/k_D = 2.2) (Fig. 4D). This result is further corroborated by findings that *N*-neopentyl PNX and PTZ, which present hindered α-CH bonds, are poorer inhibitors than either the *N*-ethyl or *N*-benzyl PNX derivatives (Fig. 3C and D). The requirement for acid to achieve highly effective inhibition must therefore lie with promoting iminium ion formation over deprotonation to yield an α-aminoalkyl radical and suppressing enamine formation when possible (*i.e.* for *N*-ethyl).[41]

To corroborate the involvement of the iminium ion in the dealkylation step of *N*-alkylated PNX (and PTZ), we synthesized and evaluated isomeric *N*-propenyl and *N*-allyl PNX derivatives, which possess distinct reactive C–H bonds, but which should lead to the same iminium ion upon oxidation (Fig. 4F). Indeed, both compounds were good inhibitors (Fig. 4E). Moreover, where both *N*-propenylPNX and *N*-allylPNX were unable to inhibit the autoxidation of BA, added acetic acid resulted in clearly inhibited autoxidations (see ESI†). Interestingly, the profile for the *N*-propenylPNX was somewhat different than that observed for the *N*-allylPNX derivative – with the former completely suppressing the autoxidation, but for a shorter period than the latter, corresponding to roughly half as many radicals trapped. Given that the *N*-propenylPNX is an enamine, we wondered if acid-catalyzed alcoholysis/hydrolysis may contribute to PNX formation, leading to the enhanced radical-trapping kinetics from the outset (due to a higher concentration of free PNX), but a shorter inhibited period (due to no radical-trapping in the dealkylation process). Indeed, we found that PNX forms from *N*-propenylPNX in the presence of acetic acid at 70 °C on the same timescale as the inhibited autoxidation (see ESI†).

With a plausible mechanism for the reactivity of the *N*-alkylated PTZ/PNX in AA, we turned our attention to the origin of the super-stoichiometric radical-trapping of the PNX/PTZ derivatives in AA. As part of the foregoing mechanistic studies where we added acetic acid to BA autoxidations inhibited by the alkylated PNX/PTZ derivatives, we did the same for autoxidations inhibited by free PNX/PTZ. In both cases, the radical-trapping stoichiometries increased – from n = 2.9 to 4.7 for PNX and from n = 2.6 to 6.8 for PTZ (see Fig. 5A).[42] Interestingly, while the autoxidations carried out in the presence of PTZ returned to the uninhibited rate after the well-defined inhibited period, the PNX-inhibited autoxidations remained retarded following the well-defined inhibited period.

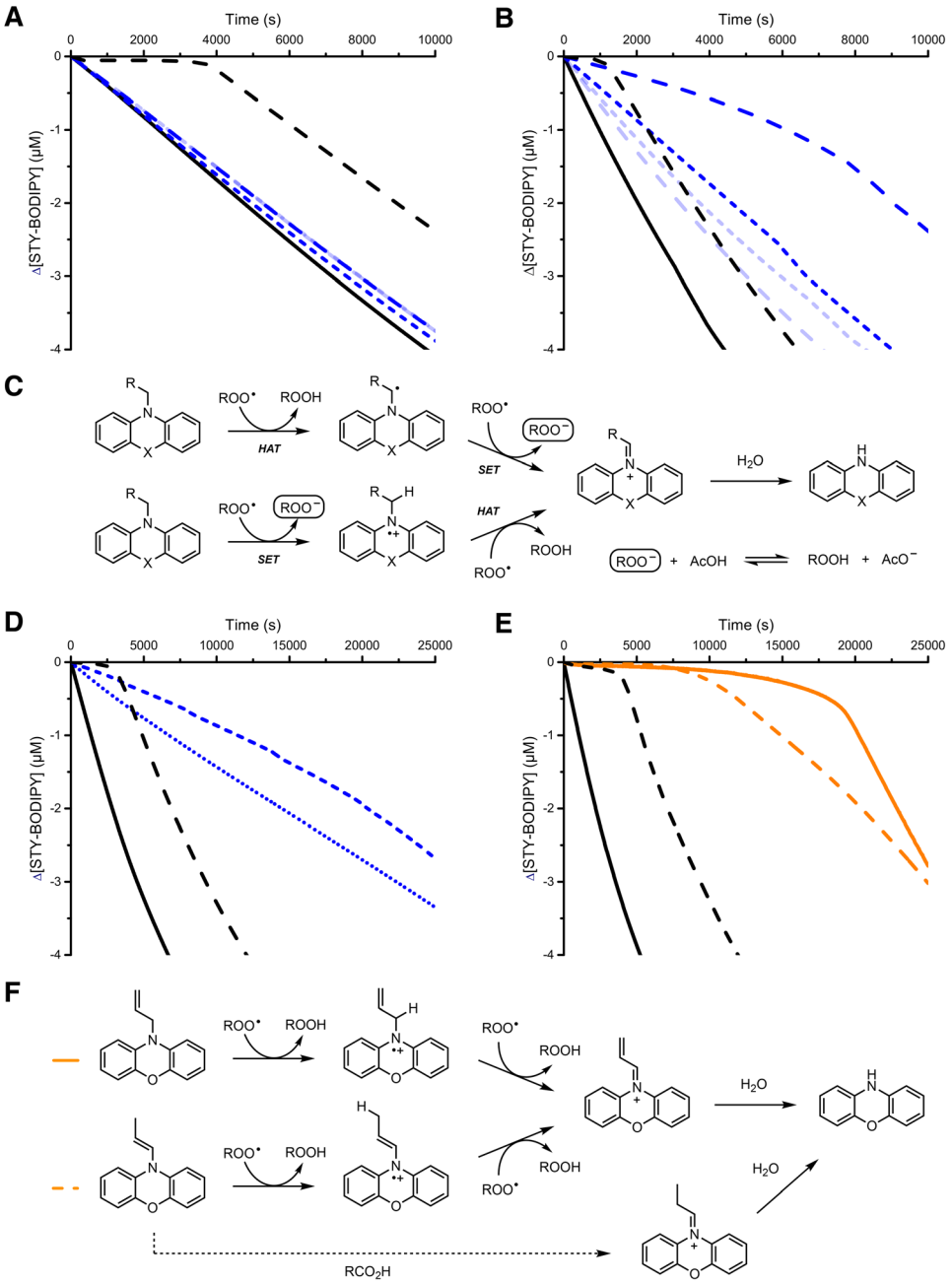

Fig. 4 (A and B). Representative co-autoxidations of BA (2.91 M) and STY-BODIPY (10 μM) initiated by di-*tert*-butylperoxide (295 mM) in chlorobenzene at 70 °C (black line) and inhibited by *N*-substituted PNX derivatives (12 μM) in the absence (A) or presence (B) of acetic acid (5.0 M). Compounds and corresponding colours are shown in Fig. 3B. STY-BODIPY consumption was monitored by absorbance at either 569 nm (A, ε = 107 571 M^{-1} cm^{-1}) or 569 nm (B, ε = 115 395 M^{-1} cm^{-1}). (C) Potential dealkylation mechanisms under the reactions conditions. (D and E) Representative co-autoxidations of AA (2.91 M) and STY-BODIPY (10 μM) initiated by di-*tert*-butylperoxide (295 mM) in chlorobenzene at 70 °C (black line) and inhibited by either *N*-C_2H_5 PNX (dashed line) or *N*-C_2D_5 PNX (dotted line) at 24 μM, and (D) either *N*-allyl PNX (solid line) or *N*-propenyl PNX (dashed line) at 24 μM (E). STY-BODIPY consumption was monitored by absorbance at 572 nm (ε = 118 469 M^{-1} cm^{-1}). (F) The dealkylation of *N*-allyl and *N*-propenyl PNX may proceed *via* the common iminium ion intermediate.

Thus, the acidic medium clearly plays a role in increasing the radical-trapping capacity of both PNX and PTZ, and whatever the mechanism, PNX can better access it.

While we have ruled out the possible intervention of the alkylperoxyl/hydroperoxyl cross-dismutation mechanism that is observed in EH (and to a lesser extent in BA), the fact that both aromatic amines display superstoichiometric activity in AA (or acidified BA) points to a mechanism involving the intervention of nitroxides. Aryl nitroxides are well-known to be produced from aromatic amines during inhibited autoxidations – most

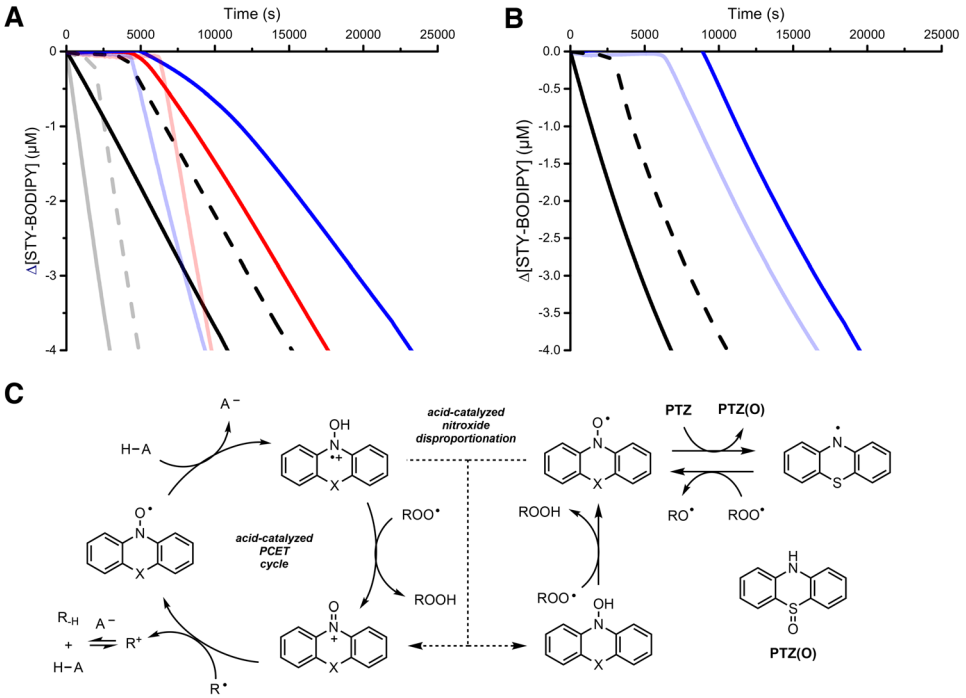

Fig. 5 (A). Representative co-autoxidations of BA (2.91 M) and STY-BODIPY (10 μM) initiated by di-*tert*-butylperoxide (295 mM) in chlorobenzene at 70 °C (black line) and inhibited by 12 μM of PNX (blue line), PTZ (red line) and PMC (black dashed line) in the absence (solid lines) or presence (semi-transparent lines) of acetic acid (5.0 M). STY-BODIPY consumption was monitored by absorbance at either 569 nm (ε = 107 571 M^{-1} cm^{-1}, solid lines) or 569 nm (ε = 115 395 M^{-1} cm^{-1}, semi-transparent lines). (B) Representative co-autoxidations of AA (2.91 M) and STY-BODIPY (10 μM) initiated by di-*tert*-butylperoxide (295 mM) in chlorobenzene at 70 °C (black line) and inhibited by 24 μM PNX (solid blue line), PNX *N*-oxyl (semi-transparent blue line) and PMC (black dashed line). STY-BODIPY consumption was monitored by absorbance at 572 nm (ε = 118 469 M^{-1} cm^{-1}). (C) Mechanistic possibilities for the super-stoichiometric radical-trapping observed for PNX and/or the nitroxide derived therefrom, and why this may be less efficient for PTZ (oxidation to the *S*-oxide, PTZ(O)).

recently in our own work with PNX.[30] Furthermore, acid has been shown to accelerate reactions of peroxyl radicals[43] – particularly with nitroxides[44] – according to the mechanism shown in Fig. 5C (left).[45] Indeed, the nitroxide derived from PNX is able to inhibit AA autoxidation similarly to PNX when added directly (Fig. 5B), but with lower stoichiometry (n = 3.6) which is reasonable given that radical-trapping by PNX is required to convert it to the nitroxide. Since nitroxides can also disproportionate to hydroxylamine and oxoammonium ions under acidic conditions,[46] the superstoichiometric radical-trapping may also result from trapping of chain-propagating radicals by HAT from the hydroxylamine or SET to oxoammonium ions, regenerating nitroxide, respectively (Fig. 5C, middle). Indeed, in preparative experiments, we found that the PNX nitroxide could be converted to PNX and phenoxazinone in the presence of acetic acid at 70 °C (see ESI†).

It remains to discuss an important finding overshadowed by the mechanistic discussion above; while PTZ and PNX had similar inhibited periods in AA, the *N*-alkylated PNXs were demonstrably better inhibitors than the corresponding *N*-alkylated PTZs. Moreover, the *N*-alkylated PNXs were characterized by much longer inhibited periods than PNX itself – which exceed the increase expected simply from the two additional radicals that would be trapped in the dealkylation process. Since the PNX-derived nitroxide is known to rapidly accumulate when PNX is used to inhibit autoxidations – in part due to the direct reaction of PNX with O_2 at elevated temperatures[30] – disproportionation competes with acid-catalyzed radical-trapping since its kinetics are bimolecular in nitroxide. Use of the more slowly reacting PNX precursors that require dealkylation to form PNX *in situ* would be expected to lead to lower levels of nitroxide at any given time, minimizing disproportionation. Nitroxide does not accumulate to the same extent from PTZ because it is both less reactive *and* any nitroxide that does form can react with starting PTZ to yield the corresponding *S*-oxide[30] (Fig. 5C, right) – minimizing nitroxide disproportionation and accounting for similar (if not slightly longer) inhibited periods observed for (unalkylated) PTZ relative to PNX in AA. Yet, since PNX is more inherently reactive than PTZ, PNX formed slowly from its *N*-alkylated precursors *in situ* will be better able to inhibit autoxidation than PTZ formed slowly from its *N*-alkylated precursors. These results suggest that *N*-alkylated PNX derivatives should be explored further as stabilizers for AA.

Conclusions

The STY-BODIPY co-autoxidation approach has been employed to monitor the inhibition of autoxidation of AA and its esters

by RTAs and has been parameterized to quantitate both radical-trapping kinetics and stoichiometry. These studies have revealed stark differences in the radical-trapping activity of conventional phenolic, aminic and nitroxide RTAs as a function of substrate. These differences are based on whether the RTA can catalyze hydroperoxyl/alkylperoxyl dismutation in substrates where hydroperoxyl is readily formed as part of the autoxidation, or whether acid is present to catalyze the reactions of nitroxides with peroxyl radicals. Data obtained with PTZ – which is generally used to stabilize AA from runaway polymerization – and *N*-alkylated derivatives thereof suggest that the accepted radical-trapping mechanism is unlikely to operate (at least in the presence of O_2) and a new mechanism is proposed that is consistent with the available data. *N*-Alkylated PNXs appear to be privileged inhibitors, which not only outperform PTZ and *N*-alkylated derivatives thereof, but also phenolic and other aminic and nitroxide RTAs.

Experimental section

General

All chemicals and solvents were purchased from commercial suppliers and used without further purification unless otherwise indicated except EH, BA and AA. BA and AA were distilled twice at 50 to 60 °C under 10 mbar vacuum. The purified material could be kept at −20 °C for up to 5 days. EH was percolated through a column of basic alumina immediately before use. STY-BODIPY,[15] the *N*-alkylated phenoxazines and phenothiazines,[47] hydroquinones[48] and phenoxazine-*N*-oxyl[30] were synthesized similarly to previous reports and purified by column chromatography using flash silica gel (230–400 mesh) as described in detail in the ESI.† ^{1}H and ^{13}C NMR were recorded on Bruker AVANCE spectrometers operating at either 600, 400 or 300 MHz. High resolution mass spectra were obtained on a Kratos Concept Tandem mass spectrometer.

Inhibited co-autoxidations of STY-BODIPY and EH

To a 3 mL cuvette were added EH (1.14 mL) and chlorobenzene (1.16 mL). After equilibration for 5 minutes at 70 °C, the cuvette was blanked, and to the cuvette were added STY-BODIPY (15 μL of 1.74 mM solution in DMSO) and DTBP (235 μL) followed by thorough mixing. The absorbance at 568 nm was monitored for 20–25 minutes to ensure linear reaction progress, after which inhibitor (50 μL of 0.3 mM solution in TCB) was added. The solution was thoroughly mixed and the readings were resumed. The inhibition rate constant (k_{inh}) and radical-trapping stoichiometry (n) were determined according to eqn (1) and (2) in Fig. 1 and are reported ±SD from three independent experiments.

Inhibited co-autoxidations of STY-BODIPY and BA

To a 3 mL cuvette were added BA (1.0 mL) and 1,2,4-trichlorobenzene (1.15 mL). After equilibration for 5 minutes at 70 °C, the cuvette was blanked, and to the cuvette were added STY-BODIPY (14 μL of 1.74 mM solution in DMSO) and DTBP (235 μL) followed by thorough mixing. The absorbance at 569 nm was monitored for 5–10 minutes to ensure linear reaction progress, after which inhibitor (100 μL of 0.3 mM solution in TCB) was added. The solution was thoroughly mixed, and the readings were resumed. The inhibition rate constant (k_{inh}) and radical-trapping stoichiometry (n) were determined according to eqn (1) and (1) in Fig. 1 and are reported ±SD from three independent experiments.

Inhibited co-autoxidations of STY-BODIPY and AA

To a 3 mL cuvette were added 2-AA (0.5 mL) and 1,2,4-trichlorobenzene (1.85 mL). After equilibration for 5 minutes at 70 °C, the cuvette was blanked, and to the cuvette were added STY-BODIPY (15 μL of 1.74 mM solution in DMSO) and DTBP (235 μL) followed by thorough mixing. The absorbance at 572 nm was monitored for 5 minutes to ensure linear reaction progress, after whichinhibitor (200 μL of 0.3 mM solution in TCB) was added. The solution was thoroughly mixed, and the readings were resumed. The inhibition rate constant (k_{inh}) and radical-trapping stoichiometry (n) were determined according to eqn (1) and (1) in Fig. 1 and are reported ±SD from three independent experiments.

Electrochemistry

Standard potentials were measured by cyclic voltammetry at 25 °C in dry acetonitrile (3.0 mM amine) containing Bu_4NPF_6 (0.1 M) as electrolyte. Experiments were carried out with a potentiostat equipped with a glassy-carbon working electrode, a platinum auxiliary electrode and $Ag/AgNO_3$ (0.005 M) reference electrode. The given E° were determined relative to the ferrocene/ferrocenium couple measured under the same conditions (Fc/Fc^+ *vs.* NHE +0.64 V).

Author contributions

OSN, OG and DAP designed the experiments. OSN synthesized all compounds as reported in the ESI† and carried out all experiments related to the inhibited autoxidations. OSN wrote the first draft of the manuscript, which was subsequently edited by DAP and OG.

Data availability

The data supporting this article have been included as part of the ESI.†

Conflicts of interest

There are no conflicts to declare.

Acknowledgements

We gratefully acknowledge financial support of BASF SE (Ludwigshafen) and Dr A. Upadhyay for technical assistance.

References

1 E. V. Makshina, J. Canadell, J. van Krieken, E. Peeters, M. Dusselier and B. F. Sels, *ChemCatChem*, 2019, **11**, 180–201.
2 Acrylic Acid Market Analysis. **https://www.chemanalyst.com/industry-report/acrylic-acid-market-287**.
3 N. Ballard and J. M. Asua, *Prog. Polym. Sci.*, 2018, **79**, 40–60.
4 R. Saada, D. Patel and B. Saha, *Process Saf. Environ. Prot.*, 2015, **97**, 109–115.
5 C. S. Kao and K. H. Hu, *J. Loss Prev. Process Ind.*, 2002, **15**, 213–222.
6 O. S. Privett, *J. Am. Oil Chem. Soc.*, 1959, **36**, 507–512.
7 T. Pirman, M. Ocepek and B. Lizokar, *Ind. Eng. Chem. Res.*, 2021, **60**, 9347–9367.
8 N. N. Pozdeeva and E. T. Denisov, *Kinet. Catal.*, 2010, **51**, 211–218.
9 L. M. Smith, H. M. Aitken and M. L. Coote, *Acc. Chem. Res.*, 2018, **51**, 2006–2013.
10 H. Becker and H. Vogel, *Chem. Eng. Technol.*, 2006, **29**, 1227–1231.
11 H. Becker and H. Vogel, *Chem. Eng. Technol.*, 2006, **29**, 931–936.
12 K. U. Ingold and D. A. Pratt, *Chem. Rev.*, 2014, **114**, 9022–9046.
13 L. B. Levy, *J. Polym. Sci., Part A:Polym. Chem.*, 1985, **23**, 1505–1515.
14 S. Schulze and H. Vogel, *Chem. Eng. Technol.*, 1998, **21**, 829–837.
15 E. A. Haidasz, A. T. M. Van Kessel and D. A. Pratt, *J. Org. Chem.*, 2016, **81**, 737–744.
16 J. Helberg and D. A. Pratt, *Chem. Soc. Rev.*, 2021, **50**, 7343–7358.
17 M. S. Blois, *Nature*, 1958, **181**, 1199–1200.
18 R. Re, N. Pellegrini, A. Proteggente, A. Pannala, M. Yang and C. R. Evans, *Free Radicals Biol. Med.*, 1999, **26**, 1231–1237.
19 G. W. Burton and K. U. Ingold, *Acc. Chem. Res.*, 1986, **19**, 194–201.
20 E. T. Denisov and I. B. Afanas'ev, Oxidation and Antioxidants in Organic Chemistry and Biology; Taylor and Francis group ed.; CRC Press: Boca Raton, FL, 2005; Section 29.5 (the value of $2k_t$ of isopropanol has been taken as a reference for 2-EH at 60 °C).
21 L. Valgimigli and D. A. Pratt, *Acc. Chem. Res.*, 2015, **48**, 966–975.
22 L. A. Farmer, E. A. Haidasz, M. Griesser and D. A. Pratt, *J. Org. Chem.*, 2017, **82**, 10523–10536.
23 J. A. Howard and K. U. Ingold, *Can. J. Chem.*, 1967, **45**, 785–792.
24 J.-F. Poon and D. A. Pratt, *Acc. Chem. Res.*, 2018, **51**, 1996–2005.
25 K. A. Harrison, E. A. Haidasz, M. Griesser and D. A. Pratt, *Chem. Sci.*, 2018, **9**, 6068–6079.
26 L. Valgimigli, R. Amorati, M. G. Fumo, G. A. DiLabio, G. F. Pedulli, K. U. Ingold and D. A. Pratt, *J. Org. Chem.*, 2008, **73**, 1830–1841.
27 M. S. Akhlaq, C. P. Murthy, S. Steenken and C. Van Sonntag, *J. Phys. Chem.*, 1989, **93**, 4331–4334.
28 E. T. Denisov, *Chem. Rev.*, 1987, **87**, 1313–1357.
29 A. Baschieri, L. Valgimigli, S. Gabbanini, G. A. DiLabio, E. R. Montalvo and R. Amorati, *J. Am. Chem. Soc.*, 2018, **140**, 10354–10362.
30 J.-F. Poon, L. A. Farmer, E. A. Haidasz and D. A. Pratt, *Chem. Sci.*, 2021, **12**, 11065–11079.
31 A. Baschieri, R. Amorati, L. Valgimigli and L. Sambri, *J. Org. Chem.*, 2019, **84**(21), 13655–13664.
32 L. B. Levy, *J. Polym. Sci., Part A:Polym. Chem.*, 1992, **30**, 569–576.
33 J. Mosnáček, R. Nicolaÿ, K. K. Kar, S. O. Fruchey, M. D. Cloeter, R. S. Harner and K. Matyjaszewski, *Ind. Eng. Chem. Res.*, 2012, **51**, 3910–3915.
34 C. Iuga, A. Campero and A. V. Bunge, *RSC Adv.*, 2015, **5**, 14678–14689.
35 M. H. Abraham, P. L. Grellier, D. V. Prior, J. J. Morris and P. J. Taylor, *J. Chem. Soc., Perkin Trans. 2*, 1990, 521–529.
36 M. Lucarini, P. Pedrielli, G. F. Pedulli, L. Valgimigli, D. Gigmes and P. Tordo, *J. Am. Chem. Soc.*, 1999, **121**, 11546–11155.
37 L. A. Farmer, E. A. Haidasz, M. Griesser and D. A. Pratt, *J. Org. Chem.*, 2017, **82**, 10523–10536.
38 A. A. Zavitsas and C. Chatgilialoglu, *J. Am. Chem. Soc.*, 1995, **117**, 10645–10654.
39 B. Maillard, K. U. Ingold and J. C. Scaiano, *J. Am. Chem. Soc.*, 1983, **105**, 5095–5099.
40 B. A. Kowert, L. Marcoux and A. J. Bard, *J. Am. Chem. Soc.*, 1972, **94**, 5538–5550.
41 It is possible that in the preparative reaction where there is no substrate (*i.e.* just AIBN and acid) that dealkylation proceeds *via* a chain reaction. However, in the presence of substrate, it is unlikely that the peroxyl radical derived from O_2 addition to the α-aminoalkyl radical would react with *N*-benzylPNX over substrate given the massive concentration difference.
42 Interestingly, we find that the rate of initiation increases in BA in the presence of acetic acid (1.2×10^8 nM s^{-1}), as evident from the shorter inhibited periods for PMC. This largely ecapitulates the increased rate of initiation observed in AA (1.5×10^8 nM s^{-1}) relative to BA (6.9×10^9 nM s^{-1}).
43 L. Valgimigli, R. Amorati, S. Petrucci, G. F. Pedulli, D. Hu, J. J. Hanthorn and D. A. Pratt, *Angew. Chem., Int. Ed.*, 2009, **48**, 8348–8351.
44 R. Amorati, G. F. Pedulli, D. A. Pratt and L. Valgimigli, *Chem. Commun.*, 2010, **46**, 5139–5141.
45 E. A. Haidasz, D. Meng, R. Amorati, A. Baschieri, K. U. Ingold, L. Valgimigli and D. A. Pratt, *J. Am. Chem. Soc.*, 2016, **138**, 5290–5298.

46 (*a*) G.-J. ten Brink, I. W. C. E. Arends and R. A. Sheldon, *Science*, 2000, **287**, 1636; (*b*) R. A. Sheldon, I. W. C. E. Arends, G.-J. ten Brink and A. Dijksman, *Acc. Chem. Res.*, 2002, **35**, 774; (*c*) F. Minisci, F. Recupero, A. Cecchetto, C. Gambarotti, C. Punta, R. Faletti, R. Paganelli and G. F. Pedulli, *Eur. J. Org. Chem.*, 2004, **109**, 109–119; (*d*) V. D. Sen and V. A. Golubev, *J. Phys. Org. Chem.*, 2009, **22**, 138.

47 (*a*) J. Mosnáček, R. Nicolaÿ, K. K. Kar, S. O. Fruchey, M. D. Cloeter, R. S. Harner and K. Matyjaszewski, *Ind. Eng. Chem. Res.*, 2012, **51**, 3910–3915; (*b*) D.-G. Chen, Y. Chen, C.-H. Wu, Y.-A. Chen, M.-C. Chen, J.-A. Lin, C.-Y. Huang, J. Su, H. Tian and P.-T. Chou, *Angew. Chem.*, 2019, **131**, 13431–13435; (*c*) G. K. Musorin, *Russ. J. Org. Chem.*, 2003, **39**, 915–918; (*d*) P. Borowicz, J. Herbich, A. Kapturkiewicz, R. A-Ostrowska, J. Nowacki and G. Grampp, *Phys. Chem. Chem. Phys.*, 2000, **2**, 4275–4280; (*e*) P. R. Castillo and S. L. Buchwald, *Chem. Rev.*, 2016, **116**, 12564–12649.

48 V. A. Timoshchuk and R. I. Hogrefe, *Nucleosides, Nucleotides Nucleic Acids*, 2009, **28**, 464–472.